ACCSCIENCE PUBLISHING

Advanced Neurology

RESEARCH ARTICLE

3D bioprinting of patient-derived cholangiocarcinoma organoids in a decellularized liver matrix-based bioink for drug testing

Supplementary Files

Table S1. Clinicopathological characteristics of patient-derived CCA organoid lines

Line ID	CCA subtype	Grade/differentiation	TNM stage	AJCC stage	Gem/Cis response
CCAO-1	pCCA	G3/poorly differentiated	pT1N1M0	IIIC	SD
CCAO-2	dCCA	G2/moderately differentiated	pT2N0M0	IIA	PR
CCAO-3	pCCA	G2/moderately differentiated	pT2N1M0	IIIC	NA

Note: All organoid lines were established from surgical tumor tissues, and all corresponding tumor specimens were histologically diagnosed as adenocarcinoma. Pathologic stage was assigned according to the AJCC 8th edition staging system based on the anatomical subtype of cholangiocarcinoma. Gem/Cis response refers to the best-documented clinical response to gemcitabine/cisplatin-based therapy in the medical records.
Abbreviations: AJCC: American Joint Committee on Cancer; CCA: Cholangiocarcinoma; CCAO: Patient-derived cholangiocarcinoma organoid; dCCA: Distal cholangiocarcinoma; Gem/Cis: Gemcitabine/cisplatin; NA: Not available; pCCA: Perihilar cholangiocarcinoma; PR: Partial response; SD: Stable disease; TNM: Tumor-node-metastasis.

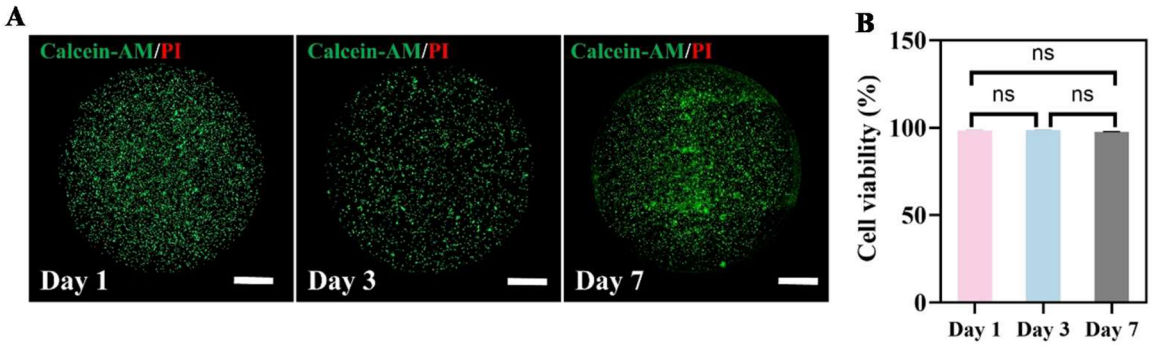

Figure S1. Biocompatibility evaluation of DLM with HepG2 cells. (A) Representative calcein-AM/PI staining images of HepG2 cells cultured in DLM on days 1, 3, and 7. Live cells are shown in green and dead cells in red. Scale bars: 3 mm. (B) Quantitative analysis of HepG2 cell viability at days 1, 3, and 7. Quantitative data are presented as mean ± standard deviation from $n = 3$ independent biological replicates unless otherwise indicated. Statistical significance is indicated as follows: ns, not significant.
Abbreviations: DLM: Decellularized liver matrix; PI: Propidium iodide.

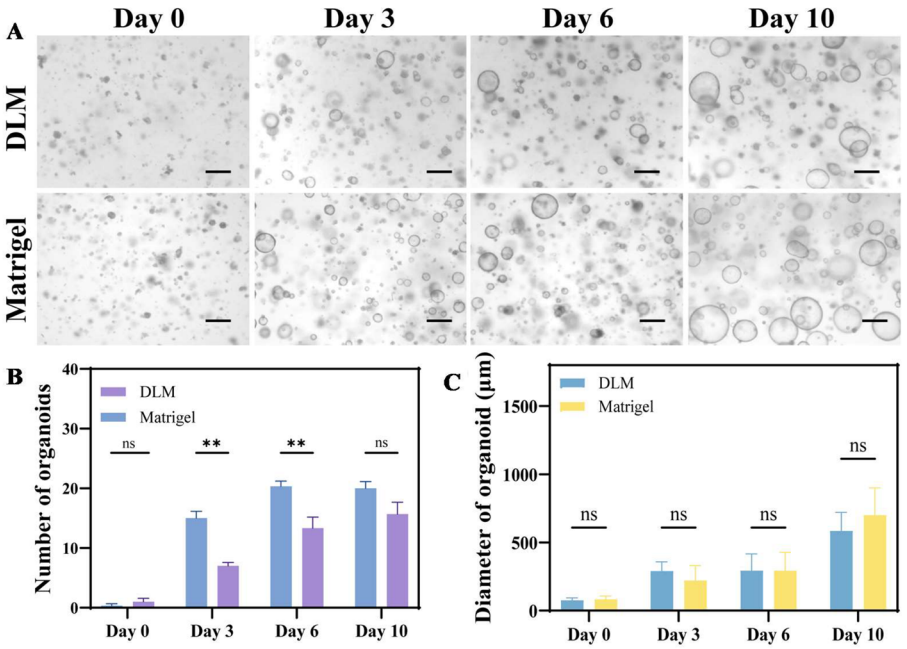

Figure S2. Comparison of normal mouse liver organoid growth in decellularized liver matrix (DLM) hydrogel and Matrigel. Representative bright-field images of mouse liver organoids cultured in DLM hydrogel or Matrigel at days 0, 3, 6, and 10. Scale bar: 300 μm (A). Quantitative analyses of organoid number (B) and organoid diameter (C) at different culture time points are shown in the lower panels. Data are presented as mean ± standard deviation. Quantitative data are presented as mean ± standard deviation from $n = 3$ independent biological replicates unless otherwise indicated. Statistical significance is indicated as follows: ns, not significant; $^{**}p < 0.01$.

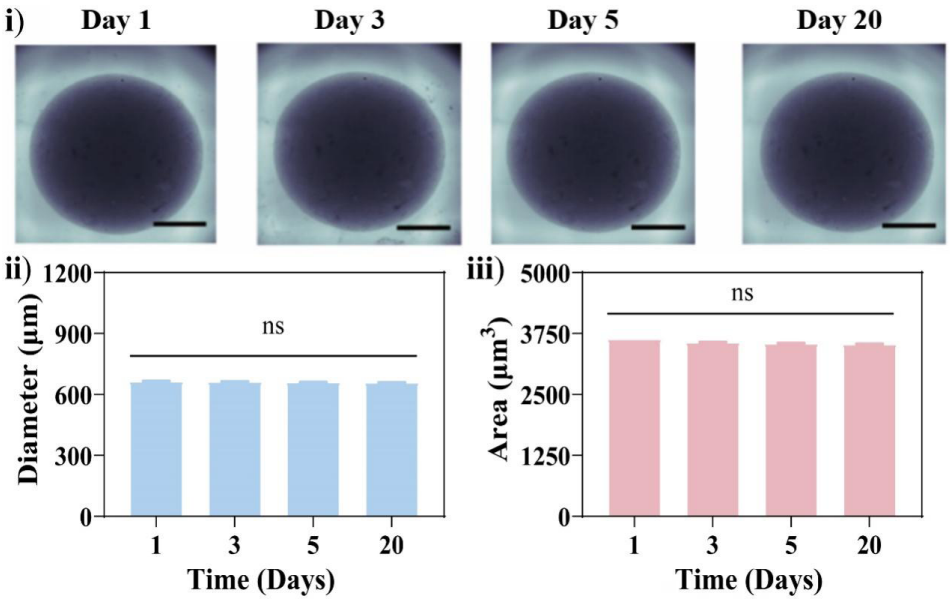

Figure S3. Stability assessment of DLM–Ru/SPS. Representative images and stability analysis of DLM–Ru/SPS over time, including (A) representative images of DLM–Ru/SPS samples on days 1, 3, 5, and 20. Scale bars: 2 mm. (B) Changes in the diameter of DLM–Ru/SPS over 20 days, and (C) changes in the area of DLM–Ru/SPS over 20 days. No significant differences were observed among the groups. Quantitative data are presented as mean ± standard deviation from n=3 independent biological replicates unless otherwise indicated. Quantitative data are presented as mean ± standard deviation from $n = 3$ independent biological replicates unless otherwise indicated. Statistical significance is indicated as follows: ns, not significant.
Abbreviations: DLM: Decellularized liver matrix; Ru: Ruthenium; SPS: Sodium persulfate.

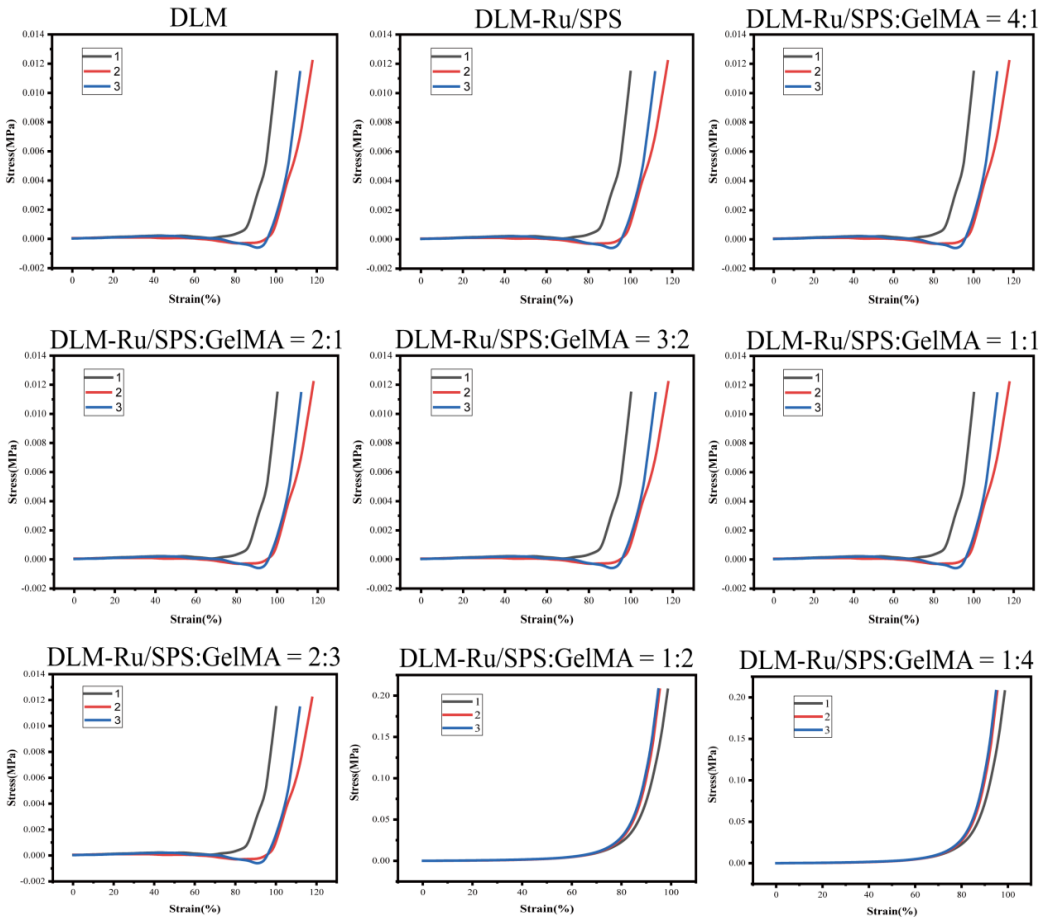

Figure S4. Representative compressive stress–strain curves of DLM-based hydrogels with different formulations. Compressive stress–strain curves of DLM, DLM–Ru/SPS, and DLM–Ru/SPS:GelMA hydrogels with different DLM-Ru/SPS:GelMA ratios, including 4:1, 2:1, 3:2, 1:1, 2:3, 1:2, and 1:4. For each hydrogel formulation, three independent samples are shown as curves 1, 2, and 3. Stress is shown in MPa and strain is shown as a percentage.
Abbreviations: DLM: Decellularized liver matrix; GelMA: Gelatin methacryloyl; Ru: Ruthenium; SPS: Sodium persulfate.

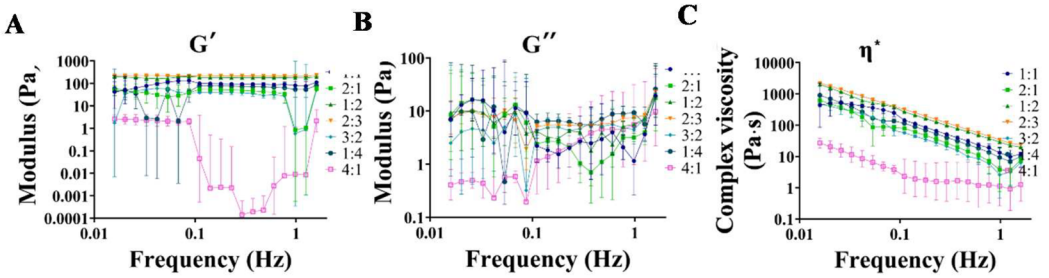

Figure S5. Frequency sweep rheological characterization of DLM–Ru/SPS:GelMA bioinks. The bioinks were prepared with different DLM–Ru/SPS-to-GelMA volumetric ratios, including 4:1, 2:1, 3:2, 1:1, 2:3, 1:2, and 1:4. (A) Storage modulus G′ as a function of frequency. (B) Loss modulus G″ as a function of frequency. (iii) Complex viscosity η* as a function of frequency. Both the horizontal and vertical axes are plotted on logarithmic scales.
Abbreviations: DLM: Decellularized liver matrix; GelMA: Gelatin methacryloyl; Ru: Ruthenium; SPS: Sodium persulfate.

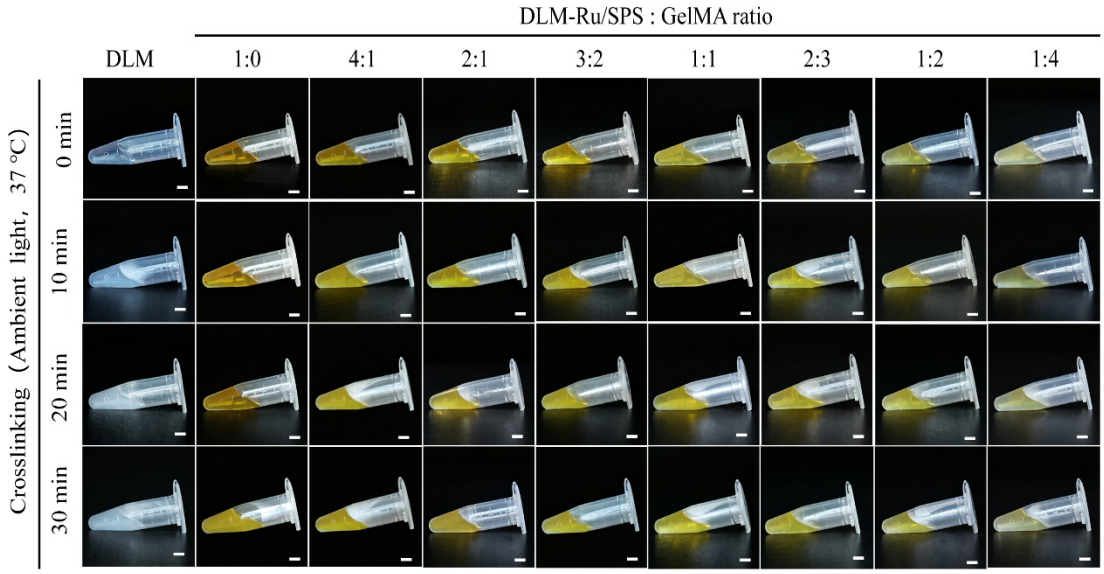

Figure S6. Photo-crosslinking behavior of DLM–Ru/SPS:GelMA hydrogels under ambient light at 37°C. Representative images showing the gelation status of DLM hydrogel and DLM–Ru/SPS:GelMA precursor solutions with different DLM–Ru/SPS:GelMA ratios, including 1:0, 4:1, 2:1, 3:2, 1:1, 2:3, 1:2, and 1:4, after exposure to ambient light at 37°C for 0, 10, 20, and 30 minutes. Gelation was assessed using the tube inversion method. DLM alone remained in a liquid-like state, whereas DLM–Ru/SPS:GelMA formulations exhibited time-dependent crosslinking and hydrogel formation, with gelation behavior varying according to the DLM–Ru/SPS:GelMA ratio. Scale bars: 5 mm.
Abbreviations: DLM: Decellularized liver matrix; GelMA: Gelatin methacryloyl; Ru: Ruthenium; SPS: Sodium persulfate.

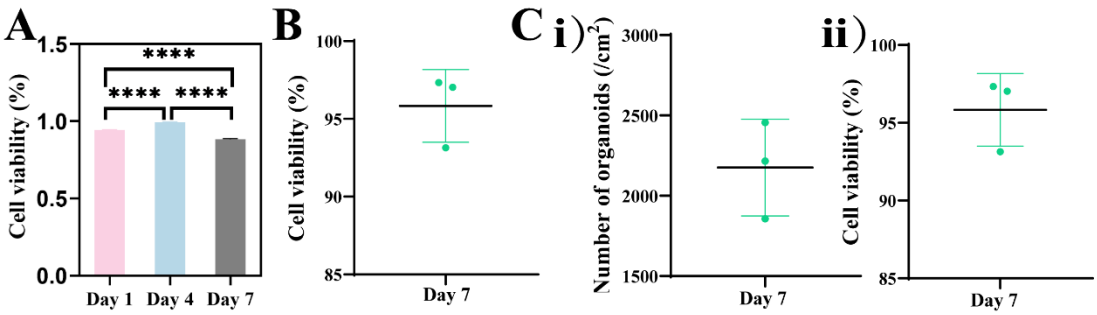

Figure S7. Viability and growth assessment of CCAOs cultured in 3D-printed DLM–Ru/SPS:GelMA hydrogels. The hydrogel was photopolymerized under 405-nm light irradiation for 50 seconds. (A) Quantitative analysis of CCOAs viability after 1, 4, and 7 days of culture in DLM–Ru/SPS:GelMA hydrogels. (B) Quantitative analysis of L929 cell viability on day 7. (C) Growth and viability evaluation of cholangiocarcinoma organoids cultured in DLM–Ru/SPS:GelMA hydrogels on day 7. (i) Quantification of organoid number per unit area. (ii) Quantitative analysis of organoid viability. Data are presented as mean ± standard deviation. Quantitative data are presented as mean ± standard deviation from n=3 independent biological replicates unless otherwise indicated. Statistical significance is indicated as follows: $^{****}p < 0.0001$.
Abbreviations: 3D: Three-dimensional; CCAO: Cholangiocarcinoma organoid; DLM: Decellularized liver matrix; GelMA: Gelatin methacryloyl; L929: Mouse fibroblast cell line L929; Ru: Ruthenium; SPS: Sodium persulfate.

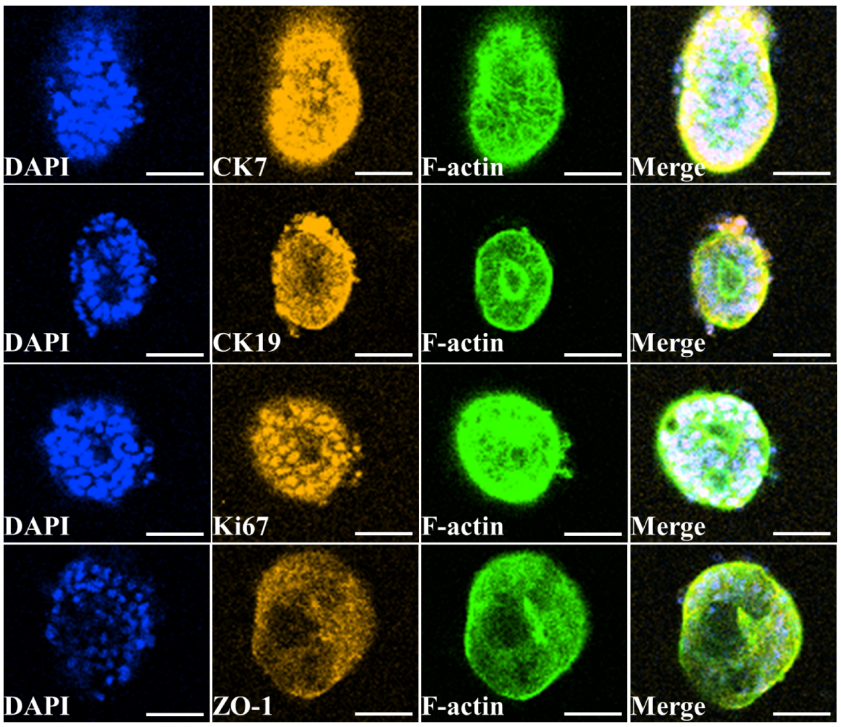

Figure S8. Two-dimensional confocal immunofluorescence images of 3D-printed hydrogels encapsulating CCAOs. Representative 2D confocal fluorescence images of CCAOs encapsulated in 3D-printed hydrogels and stained for DAPI, CK7, CK19, Ki67, ZO-1, and F-actin. Nuclei are shown in blue (DAPI), CK7, CK19, Ki67, and ZO-1 are shown in yellow, and F-actin/cytoskeleton is shown in green (phalloidin-FITC). Merged images show the spatial distribution of cholangiocarcinoma-associated epithelial markers CK7 and CK19, the proliferative marker Ki67, the tight junction marker ZO-1, and cytoskeletal organization within the organoids. These images provide complementary single-plane fluorescence characterization corresponding to Figure 5E. Scale bars: 50 μm.

Abbreviations: 2D: Two-dimensional; 3D: Three-dimensional; CCAO: Cholangiocarcinoma organoid; CK7: Cytokeratin 7; CK19: Cytokeratin 19; DAPI: 4′,6-Diamidino-2-phenylindole; F-actin: Filamentous actin; FITC: Fluorescein isothiocyanate; Ki67: Marker of proliferation Ki-67; ZO-1: Zonula occludens-1.

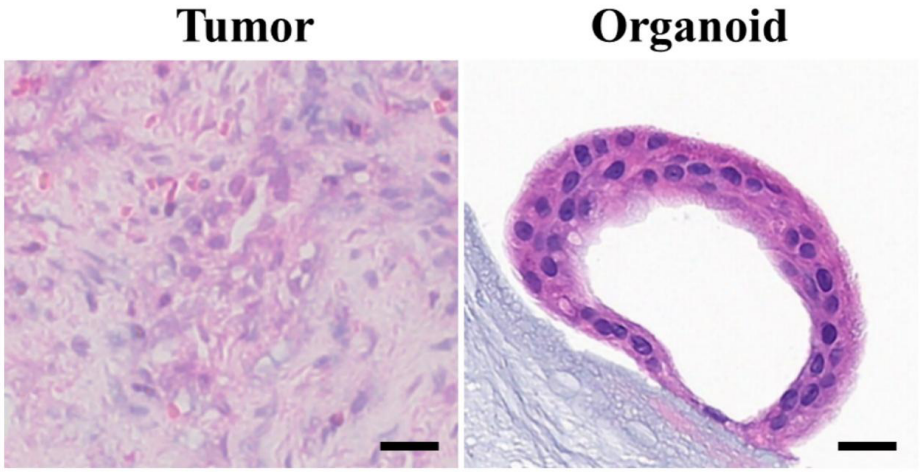

Figure S9. Histological comparison of human cholangiocarcinoma tissue and matched patient-derived organoids. Representative hematoxylin and eosin-stained sections of primary human cholangiocarcinoma tissue (tumor, left) and corresponding patient-derived cholangiocarcinoma organoids (organoid, right). Both samples were derived from human cholangiocarcinoma specimens. Nuclei are stained blue-purple, while the cytoplasm and extracellular matrix are stained pink. Scale bars: 20 μm.

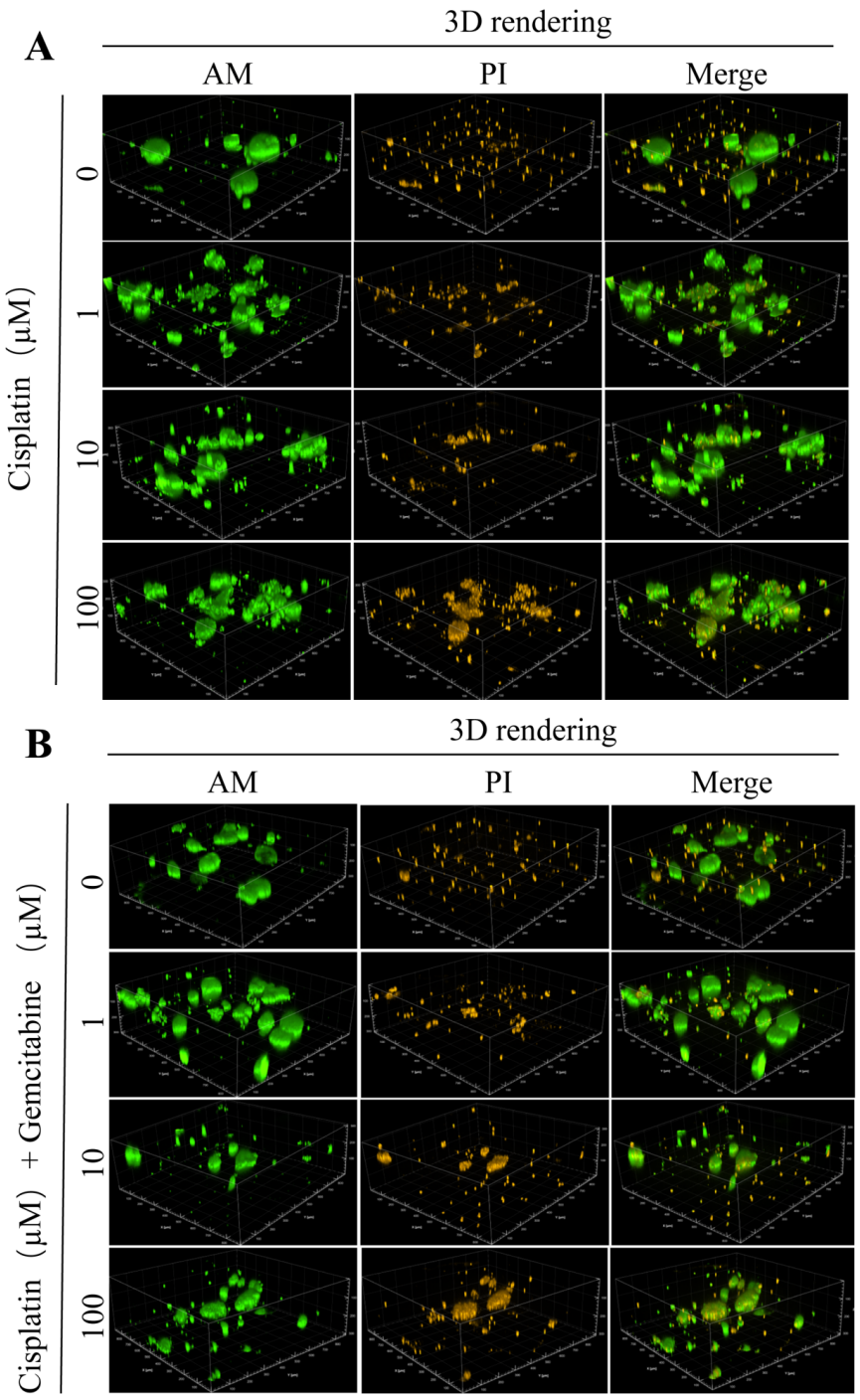

Figure S10. 3D live/dead staining of organoids after chemotherapy treatment. (A) Representative 3D-rendered fluorescence images of organoids treated with different concentrations of cisplatin, including 0, 1, 10, and 100 μM. (B) Representative 3D-rendered fluorescence images of organoids treated with cisplatin in combination with gemcitabine at the indicated concentrations, including 0, 1, 10, and 100 μM. Live and dead cells were visualized using AM and PI staining, respectively. Green fluorescence indicates live cells stained with AM, while yellow/orange fluorescence indicates PI-positive dead cells. Merged images show the overall spatial distribution of viable and dead cells within the 3D organoid structures. Images are presented as 3D renderings. Abbreviations: 3D: Three-dimensional; AM: Calcein acetoxymethyl ester; PI: Propidium iodide.

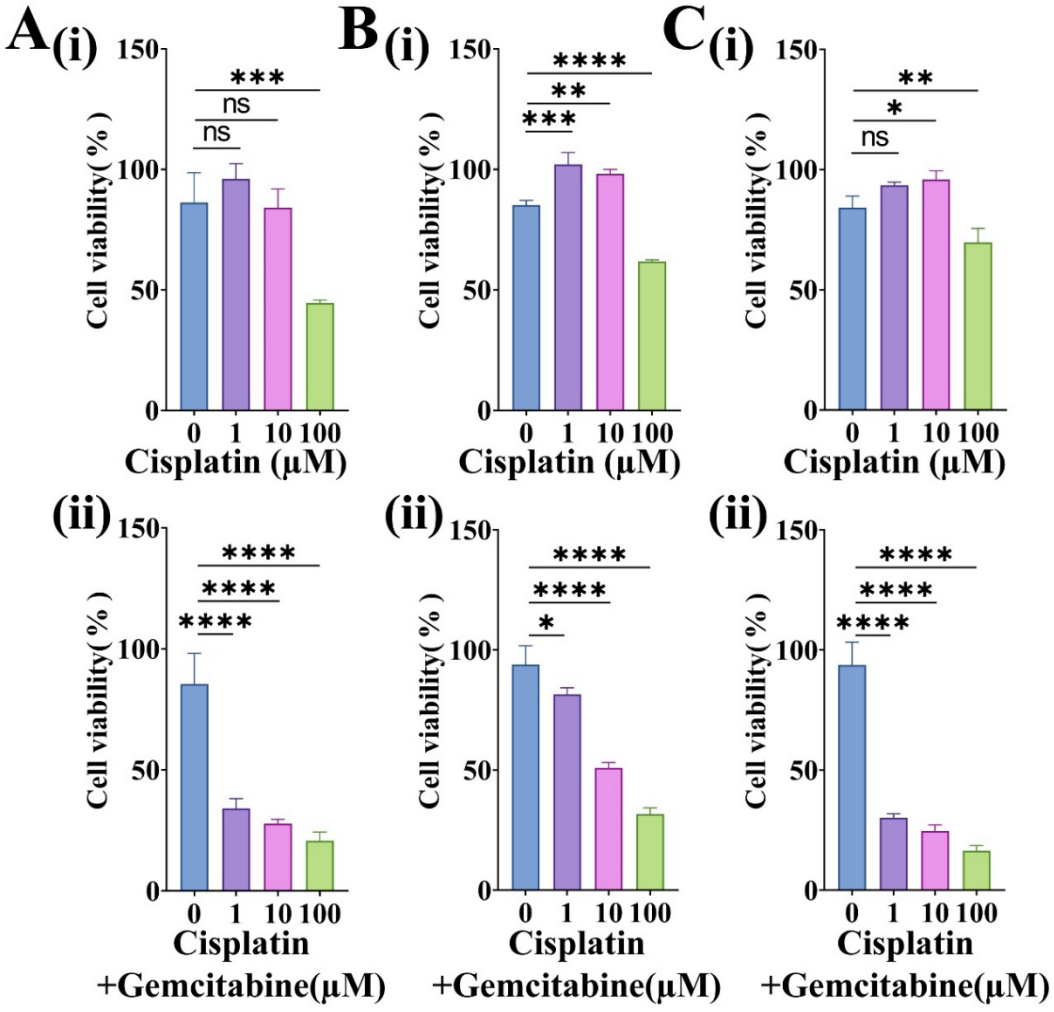

Figure S11. Drug sensitivity assessment. Cell viability was quantified based on calcein-AM/PI live/dead staining after treatment with cisplatin alone or cisplatin plus gemcitabine at concentrations of 0, 1, 10, and 100 μM for 72 hours in organoids cultured using either the traditional Matrigel culture method or the newly developed 3D-printed bioink-based drug screening platform. (A) CCAO-1 organoids cultured using the traditional Matrigel culture method. (B) CCAO-2 organoids cultured in the 3D-printed bioink-based platform. (C) CCAO-3 organoids cultured in the 3D-printed bioink-based platform. The bioink used in the 3D-printed platform was DLM–Ru/SPS:GelMA at a 4:1 ratio. Data are presented as mean ± SD. Quantitative data are presented as mean ± standard deviation from $n = 3$ independent biological replicates unless otherwise indicated. Statistical significance is indicated as follows: ns, not significant; $^{*}p < 0.05$; $^{**}p < 0.01$; $^{***}p < 0.001$; $^{****}p < 0.0001$.

Abbreviations: 3D: Three-dimensional; CCAO: Cholangiocarcinoma organoid; DLM: Decellularized liver matrix; GelMA: Gelatin methacryloyl; PI: Propidium iodide; Ru: Ruthenium; SD: Standard deviation; SPS: Sodium persulfate.